DALTON

Synthesis and structures of niobium(V) and tantalum(V) analogues of Amavadin: $[M(hida)_2]^-$ (M = Nb^V or Ta^V, H_3hida = hydroxyimino-diacetic acid) and $[Nb(R,R\text{-}hidpa)_2]^-$ [H_3hidpa = 2,2′-(hydroxyimino)-dipropionic acid]

Paul D. Smith, Spencer M. Harben, Roy L. Beddoes, Madeleine Helliwell, David Collison and C. David Garner *

Department of Chemistry, The University of Manchester, Oxford Road, Manchester M13 9PL, UK

Reactions of $M(OEt)_5$ (M = Nb or Ta) with *N*-hydroxyiminodiacetic acid (H_3hida) yielded the complexes $[M(hida)_2]^-$ (M = Nb **1** or Ta **2**). Single-crystal X-ray diffraction revealed the same novel eight-co-ordinated structure identified for Amavadin, the form in which vanadium(IV) is bound in *Amanita muscaria* mushrooms. This type of structure gives rise to chirality at the metal, where **1** and **2** consist of an equimolar mixture of the Δ and Λ helical forms in the crystal lattice. The complexes $[Nb(R,R\text{-}hidpa)_2]^-$ **3a** and $[Nb(R,S\text{-}hidpa)_2]^-$ **3b** [H_3hidpa = 2,2′-(hydroxyimino)dipropionic acid] were synthesized *via* the route used for **1** and **2**, and X-ray crystallography confirmed the presence of the same Amavadin-style geometry. Cyclic voltammetry in CH_2Cl_2 showed that at 254 K **1** and **3a** exhibit quasi-reversible reductions at $E_{\frac{1}{2}} = -1.22$ and −1.35 V (*vs.* saturated calomel electrode), respectively, whereas **2** displays an irreversible reduction (−1.92 V).

Mushrooms of the genus *Amanita* accumulate vanadium to concentrations of up to 400 mg kg^{-1} (dry weight)[1] in the form of the discrete moiety Amavadin.[2] This contains a 1:2 complex of vanadium(IV) with $hidpa^{3-}$ [H_3hidpa = 2,2′-(hydroxyimino)-dipropionic acid] which can be reversibly oxidised to the vanadium(V) level.[3] Further studies[4,5] have established that Amavadin comprises an unusual eight-co-ordinated complex, with each $hidpa^{3-}$ ligand bonding *via* the η^2-NO group and two unidentate carboxylate groups. This co-ordination environment leads to chirality at the vanadium, as shown in Scheme 1, and the isolated natural product Amavadin consists of an approximately equimolar mixture of the Δ and Λ helical forms of $[V(S,S\text{-}hidpa)_2]^{2-}$.[4,5] The $[V(hida)_2]^{2-/-}$ (H_3hida = hydroxyiminodiacetic acid) analogues have also been shown to exhibit the same Amavadin-style eight-co-ordination.[4,6–9] The unusual geometry and chemical behaviour of Amavadin has generated curiosity as to whether it is possible to extend this chemistry to include other metals. The first reported example of a chemical analogue of Amavadin was $[\Delta\text{-}Mo(R,R\text{-}hidpa)(R,S\text{-}hidpa)]^-$ and its enantiomer,[10] where molybdenum(V) is bound to two mutually *trans* η^2-NO groups and four unidentate carboxylate groups and is capable of both a one-electron reversible oxidation and a one-electron reversible reduction.[10,11] Recent studies have explored further chemical analogues of Amavadin with niobium and tantalum, leading to the synthesis of $[M(hida)_2]^-$ (M = Nb **1** or Ta **2**), $[Nb(R,R\text{-}hidpa)_2]^-$ **3a** and $[Nb(R,S\text{-}hidpa)_2]^-$ **3b**. This work has involved single-crystal X-ray diffraction to define the geometry and cyclic voltammetry to investigate redox activity, already shown to be promoted in the $[M(ligand)_2]^-$ moiety. Also ^1H and ^{13}C NMR data, in comparison with earlier studies on vanadium(V) complexes, provide valuable structural probes in solution.

Experimental

Reagents and apparatus

All reagents and solvents were obtained from normal commercial sources and used without further purification unless otherwise stated. Tetrahydrofuran (thf), Et_2O and toluene were distilled from sodium, CH_2Cl_2 distilled from CaH_2 and MeOH from magnesium, and all were stored under dinitrogen.

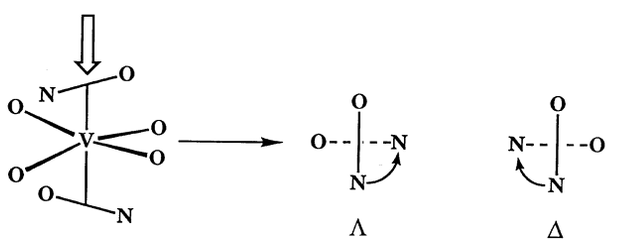

Scheme 1 Isomerism at the vanadium centre

The pro-ligands H_3hida and H_3hidpa were synthesized using a modification of the method described by Felcman *et al.*[12] Reagents were neutralised with 5 mol dm^{-3} NaOH prior to dropwise addition, followed by a further addition of 1 equivalent of NaOH, keeping the temperature below 278 K at all times, and reactions were then left to stand (*ca.* 72 h) at 275 K. The products were purified using the procedure outlined by Koch and co-workers,[13] where after the reaction period, the pro-ligands were precipitated as the zinc complex and subsequent treatment with Dowex acidic ion-exchange resin yielded the analytically pure compound as a white solid.

The salt $[NBu^n_4][BF_4]$ was prepared from $Na[BF_4]$ and $[NBu^n_4][HSO_3]$ and recrystallised from toluene.[14]

Chemical analyses were performed by the University of Manchester, Microanalytical Laboratory. Infrared spectra were recorded on a Perkin-Elmer 1710 FT spectrometer, ^1H and ^{13}C NMR spectra using a Bruker AC300 spectrometer. Samples for NMR spectroscopy in D_2O were prepared as described below, but without the addition of the $[PPh_4]^+$ cation. Mass spectra were recorded using a Kratos concept 1S spectrometer (matrix 3-nitrobenzyl alcohol). Electrochemical measurements were made with a PAR model 175 waveform generator, a model 173 potentiostat and a PAR electrochemistry cell with a three-electrode configuration consisting of a glassy carbon working electrode, a saturated calomel reference electrode (SCE) and a platinum-wire secondary electrode. Cyclic voltammograms were recorded for solutions (*ca.* 1 mmol dm^{-3}) with $[NBu^n_4][BF_4]$ (*ca.* 0.2 mol dm^{-3}) as supporting electrolyte at 254 K unless otherwise stated. All solutions were deoxygenated by bubbling dinitrogen through them for several minutes prior to use and all voltammograms were recorded with the solutions

under a dinitrogen atmosphere. All electrochemical potentials were measured relative to the SCE and were corrected for liquid-junction potentials *via* the use of the ferrocenium–ferrocene couple as an internal redox standard.[15]

Syntheses

[PPh_4][Δ,Λ-Nb(hida)$_2$] 1. The compound H_3hida (315 mg, 2.1 mmol) was added to a solution of $Nb(OEt)_5$ (318 mg, 0.25 cm^3, 1 mmol) in MeOH (10 cm^3). The reaction mixture was stirred under a dinitrogen atmosphere (*ca.* 12 h), whereupon a pale yellow solution formed. The salt [PPh_4]Br (419 mg, 1 mmol) was added, followed by Et_2O (10 cm^3) to produce a white precipitate, which was collected and dried under vacuum. This white powder was dissolved in CH_2Cl_2 (10 cm^3) and EtOH (10 cm^3) added. Colourless, tabular crystals were obtained by slow evaporation (*ca.* 72 h). Yield 270 mg, 37% (Found: C, 53.1; H, 3.95; N, 3.95. Calc. for $C_{32}H_{28}N_2NbO_{10}P$: C, 53.05; H, 3.9; N, 3.85%). IR (KBr): 1696 [ν(C=O)], 1368 [ν(C–O)] and 1130 cm^{-1} [ν(N–O)]. NMR (CD_2Cl_2, 298 K): ^{1}H, δ 7.98–7.57 (m, 20 H, Ph), 4.36, 4.26 (8 H, CH_2); ^{13}C, δ 171.40, 171.34 (CO_2^-), 136.25–117.42 (Ph), 62.19, 61.86 (CH_2). Mass spectrum (negative-ion FAB): *m/z* 385, $[Nb(hida)_2]^-$.

[PPh_4][Δ,Λ-Ta(hida)$_2$] 2. This compound was prepared as for **1** from H_3hida (315 mg, 2.1 mmol), $Ta(OEt)_5$ (406 mg, 0.26 cm^3, 1 mmol) and [PPh_4]Br (419 mg, 1 mmol). Colourless crystals were obtained from CH_2Cl_2–EtOH after slow evaporation (*ca.* 72 h). Yield 260 mg, 32% (Found: C, 47.25; H, 3.45; N, 3.45. Calc. for $C_{32}H_{28}N_2O_{10}PTa$: C, 47.3; H, 3.45; N, 3.45%). IR (KBr): 1702 [ν(C=O)], 1372 [ν(C–O)] and 1109 cm^{-1} [ν(N–O)]. NMR (CD_2Cl_2, 298 K): ^{1}H, δ 7.98–7.57 (m, 20 H, Ph), 4.45, 4.42, 4.29, 4.19 (4 d, 8 H, CH_2, $^2J_{HH}$ = −16 Hz); ^{13}C, δ 172.93, 172.82 (CO_2^-), 136.18–117.46 (Ph), 60.88, 60.69 (CH_2). Mass spectrum (negative-ion FAB): *m/z* 473, $[Ta(hida)_2]^-$.

[NEt_4][Δ,Λ-Nb(*R*,*R*-hidpa)$_2$] 3a. This compound was prepared as for **1** from *R*,*R*-H_3hidpa (368 mg, 2.1 mmol), $Nb(OEt)_5$ (318 mg, 0.25 cm^3, 1 mmol) and [NEt_4]Br (210 mg, 1 mmol). Colourless, prismatic crystals were obtained from CH_2Cl_2–thf *via* the slow liquid-diffusion technique. Yield 272 mg, 48% (Found: C, 42.2; H, 6.35; N, 7.3. Calc. for $C_{20}H_{36}N_3NbO_{10}$: C, 42.05; H, 6.35; N, 7.35%). IR (KBr): 1667 [ν(C=O)], 1381 [ν(C–O)] and 1124 cm^{-1} [ν(N–O)]. NMR (CD_2Cl_2, 298 K): ^{1}H, δ 4.54, 4.42, 4.41, 4.28 (4 q, 4 H, CH, $^3J_{HH}$ = 8), 3.21 (q, 8 H, NEt_4, $^3J_{HH}$ = 8), 1.68, 1.63, 1.56, 1.52 (4 d, 12 H, CH_3, $^3J_{HH}$ = 8) and 1.27 (t, 12 H, NEt_4, $^3J_{HH}$ = 8 Hz); ^{13}C, δ 175.58, 175.29, 174.01, 173.62 (CO_2^-), 68.12, 67.77, 64.33, 63.74 (CH), 52.41 (NEt_4), 15.03, 14.51, 12.71, 12.62 (CH_3) and 7.42 (NEt_4). Mass spectrum (negative-ion FAB): *m/z* 441, $[Nb(hidpa)_2]^-$.

[PPh_4][Δ,Λ-Nb(*R*,*S*-hidpa)$_2$] 3b. This compound was prepared as for **1** from *R*,*S*-H_3hidpa (368 mg, 2.1 mmol), $Nb(OEt)_5$ (318 mg, 0.25 cm^3, 1 mmol) and [PPh_4]Br (419 mg, 1 mmol). Colourless crystals were obtained from CH_2Cl_2–toluene *via* the slow liquid-diffusion technique. Yield 426 mg, 55% (Found: C, 55.8; H, 4.85; N, 3.3; Nb, 11.6; P, 3.75. Calc. for $C_{36}H_{36}N_2NbO_{10}P$: C, 55.4; H, 4.65; N, 3.6; Nb, 11.9; P, 3.95%). IR (KBr): 1689 [ν(C=O)], 1360 [ν(C–O)] and 1124 cm^{-1} [ν(N–O)]. NMR (CD_2Cl_2, 298 K): ^{1}H, δ 7.93–7.56 (m, 20 H, Ph), 4.49–4.22 (m, 4 H, CH) and 1.63–1.45 (m, 12 H, CH_3); ^{13}C, δ 175.66, 174.52, 174.43, 174.37, 174.29, 173.96 (CO_2^-), 136.23–117.43 (Ph), 68.63, 68.57, 68.42, 68.29, 68.20, 68.11 (CH), 16.50, 16.44, 15.43, 14.82, 12.94, 12.83 (CH_3). Mass spectrum (negative-ion FAB): *m/z* 441, $[Nb(hidpa)_2]^-$.

X-Ray crystallography

A summary of the crystallographic data for complexes **1**, **2** and **3a** is provided in Table 1. All data were corrected for Lorentz-polarisation effects and an empirical absorption correction, based on azimuthal scans of several reflections, was applied using the program DIFABS.[16] The structures were solved by direct methods.[17] Hydrogen atoms were included in the structure-factor calculations in idealised positions (C–H 0.95 Å) and assigned isotropic thermal parameters 20% greater than the equivalent *B* value of the atom to which they were bonded. The final cycle of full-matrix least squares $\Sigma w(|F_o| - |F_c|)^2$, was based on the observed reflections [$I > 3.00\sigma(I)$] and the number of variable parameters, using neutral atom scattering factors and anomalous dispersion corrections.[18] All calculations were performed using the TEXSAN[19] crystallographic software package.

Atomic coordinates, thermal parameters, and bond lengths and angles have been deposited at the Cambridge Crystallographic Data Centre (CCDC). See Instructions for Authors, *J. Chem. Soc., Dalton Trans.*, 1997, Issue 1. Any request to the CCDC for this material should quote the full literature citation and the reference number 186/336.

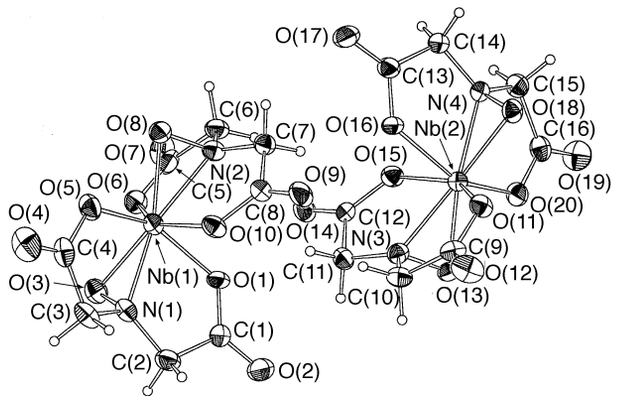

Fig. 1 Structure of the anions present in the asymmetric unit of [PPh_4][Δ,Λ-Nb(hida)$_2$]

Results and Discussion

The H_3hida and H_3hidpa pro-ligands were synthesized from bromoacetic and 2-bromopropionic acid, respectively, as reported in the literature.[12,13] However, a few modifications were made to these procedures in order to increase the yield and to optimise purity. The commercially available $M(OEt)_5$ (M = Nb or Ta) provided convenient starting materials for reactions with these pro-ligands, since earlier reactions with vanadium and molybdenum worked well with reagents containing exclusively O-donors. Herein the characterisation of further examples of chemical analogues of Amavadin are reported.

Crystallography

Compound **1**, containing a 1:2 complex of niobium(v) with $hida^{3-}$, was isolated as colourless, tabular crystals in the non-centrosymmetric space group $Pca2_1$ (Table 1). This space group possesses glide planes and there are molecules of both hands, rather than the simpler situation of $[V(hida)_2]^-$ where only one hand is obtained.[4,6] Refinement was carried for each Δ and Λ helical form at the metal and both isomers are independently present in the asymmetric unit, as shown in Fig. 1. The opposite enantiomeric arrangement of the molecules in the cell was also computed and found to refine less well. Both Δ and Λ anions in the asymmetric unit have the same overall structure as found in Amavadin,[4,5] $[V(hida)_2]^{2-/-}$,[4,6,9] and $[Mo(hidpa)_2]^-$,[10,11] with the niobium co-ordinated to two mutually *trans* η^2-NO groups and four unidentate carboxylate groups. The molecules in the asymmetric unit are of opposite hand and aligned as if an approximate *b* glide were present (Fig. 1).

The Nb–O and Nb–N bonds are each slightly longer (range 0.16–0.03; average 0.088 Å) (Table 2) than in the $[V(hida)_2]^-$

Table 1 Crystal data for compounds **1**, **2** and **3a***

	1	**2**	**3a**
Empirical formula	$C_{32}H_{28}N_2NbO_{10}P$	$C_{32}H_{28}N_2O_{10}PTa$	$C_{20}H_{36}N_3NbO_{10}$
M	724.46	812.50	571.42
Crystal colour, habit	Colourless, tabular	Colourless, needle	Colourless, prismatic
Crystal dimensions/mm	0.13 × 0.25 × 0.34	0.03 × 0.05 × 0.35	0.13 × 0.32 × 0.33
Space group	$Pca2_1$ (no. 29)	$Pca2_1$ (no. 29)	$P2_12_12_1$ (no. 19)
a/Å	22.68(2)	22.733(5)	11.862(4)
b/Å	9.822(3)	9.868(2)	20.570(8)
c/Å	27.463(7)	27.529(2)	10.594(5)
U/Å^3	6119(10)	6175(2)	2585(2)
Z	8	8	4
D_c/g cm^{-3}	1.573	1.748	1.468
μ/cm^{-1}	Cu-Kα, 43.02	Cu-Kα, 75.75	Mo-Kα, 4.97
Diffractometer	Rigaku AFC 5R	Rigaku AFC 5R	Rigaku AFC 6S
Radiation (λ/Å)	Cu-Kα (1.541 78)	Cu-Kα (1.541 78)	Mo-Kα (0.710 69)
T ± 1 K	294	296	299
Scan rate/° min^{-1}	8.0 (2 rescans)	8.0 (2 rescans)	2.0 (3 rescans)
Scan width	0.89 + 0.30 tan θ	1.21 + 0.30 tan θ	1.68 + 0.30 tan θ
$2\theta_{max}$/°	120.3	120.2	50.0
Decay (%)	7.25	7.75	0.64
No. reflections measured	5100	5252	2612
No. observations [$I > 3.00\sigma(I)$]	4126	4203	1817
No. variables	828	829	307
R, *R*′	0.033, 0.041	0.045, 0.054	0.062, 0.087
Goodness of fit	1.44	1.75	3.06

* Details in common: orthorhombic; ω–2θ scans; weighting scheme $w = 1/[\sigma^2(F_o) + x|F_o|^2]$ where $x = 0.00002$ **1**, 0.00022 **2** or 0.0022 **3a**.

Table 2 Comparison of selected metal–ligand dimensions for anions of **1**, **2**, **3a** and related vanadium analogues

	1 (M = Nb)		**2** (M = Ta)		**3** (M = Nb)	$[V(hida)_2]^-$	$[V(S,S\text{-hidpa})_2]^-$
	Δ,Λ	Λ,Δ	Δ,Λ	Λ,Δ	Λ	Λ (refs. 4, 6)	Δ (ref. 4)
M–O(1)	2.043(6)		2.01(1)		2.07(1)	1.991(7)	1.993(9)
M–O(5)	2.061(6)		2.06(1)		2.04(1)	1.955(7)	1.96(1)
M–O(6)	2.050(5)		2.04(1)		2.04(1)	1.922(8)	1.977(9)
M–O(10)	2.075(5)		2.06(1)		2.06(1)	1.936(7)	1.941(9)
M–O(3)	2.017(5)		2.017(9)		2.02(1)	1.963(8)	1.926(9)
M–O(8)	2.028(5)		2.03(1)		2.03(1)	1.977(8)	1.973(9)
M–N(1)	2.096(6)		2.13(1)		2.11(1)	2.016(8)	2.02(1)
M–N(2)	2.131(6)		2.16(1)		2.10(1)	2.028(9)	2.00(1)
M–O(11)		2.034(5)		2.12(1)			
M–O(15)		2.085(5)		2.04(1)			
M–O(16)		2.085(5)		2.02(1)			
M–O(20)		2.023(5)		2.104(9)			
M–O(13)		1.997(5)		2.00(1)			
M–O(18)		2.027(5)		2.010(9)			
M–N(3)		2.108(6)		2.10(1)			
M–N(4)		2.131(6)		2.12(1)			
O(3)–M–N(1)	39.8(2)		40.1(4)		39.4(4)	40.2(3)	41.2(4)
O(8)–M–N(2)	39.7(2)		40.7(4)		39.7(5)	40.0(3)	39.9(4)
O(13)–M–N(3)		40.2(2)		40.7(4)			
O(18)–M–N(4)		39.3(2)		39.9(4)			

counterpart. The η^2-NO groups subtend angles at the niobium which compare with the range observed for the related vanadium species (Table 2). The Δ and Λ isomers of $[Nb(hida)_2]^-$ in the asymmetric unit are structurally distinct and have a corresponding enantiomeric pair in the unit cell. The key structural features included in this discussion are labelled initially with the hand present in the asymmetric unit followed by its enantiomer. Deviations are observed with respect to the dihedral angles between the planes of the {NbNO} groups (Δ,Λ 98.3, Λ,Δ 95.1°), in contrast to the equivalent planes in the $[V(hida)_2]^-$ analogue which are inclined at 93.4°.[4,6] Fig. 2 illustrates the dihedral angle observed between the planes of the {NbNO} groups for Δ,Λ-**1**, where the angles between the N and O atoms are >90°. This deviation from 90° brings the two N atoms from each plane closer together. The variation in this dihedral angle is observed when comparing the structures obtained for the $[\Delta\text{-}V(S,S\text{-hidpa})_2]^{2-/-}$ anions, where a deviation of 4.5° is detected on oxidation from vanadium-(IV) to -(V).[5] The planes of the two {NbNO} groups in each anion are almost perpendicular (Δ,Λ 88.0 and 91.2, Λ,Δ 92.1 and 89.5°) to the least-squares plane of the niobium and four oxygen donor atoms of the unidentate carboxylate groups. These oxygen atoms are displaced from this NbO_4 least-squares plane. In Δ,Λ O(1) and O(5) sit below (−0.43 and −0.36 Å, respectively) and O(6) and O(10) sit above (0.37 and 0.45 Å, respectively) and for Λ,Δ O(11) and O(15) sit below (−0.32 and −0.48 Å, respectively) and O(16) and O(20) above (0.45 and 0.35 Å, respectively) the plane, which contains the niobium atom. Thus the carboxylate oxygen atoms from the same ligand are mutually *trans* and occupy sites on the same side of the least-squares plane thereby forming an alternation on the positions of these oxygen atoms with respect to the plane.

Compound **2** crystallises as colourless needles which are isomorphous with **1**, see Table 1 and Fig. 3. The tantalum–ligand bond lengths are comparable to those in **1** (Table 2), and again

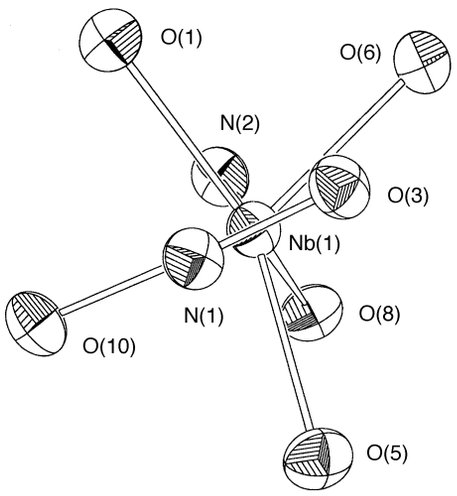

Fig. 2 View looking down the planes of the two {NbNO} groups for compound Δ,Λ-**1**

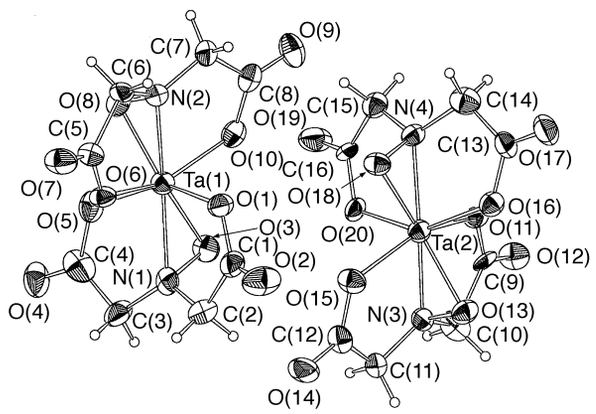

Fig. 3 Structure of the anions present in the asymmetric unit of $[PPh_4][\Delta,\Lambda\text{-Ta(hida)}_2]$

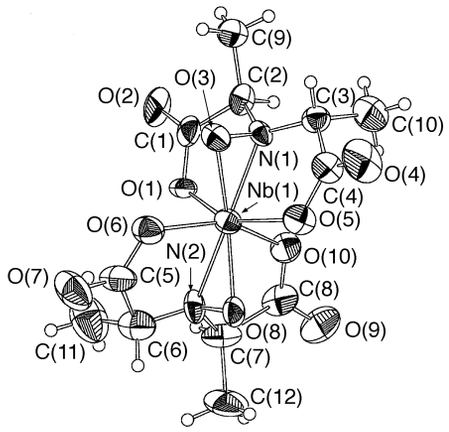

Fig. 4 Structure of the anion in $[NEt_4][\Lambda\text{-Nb}(R,R\text{-hidpa})_2]$

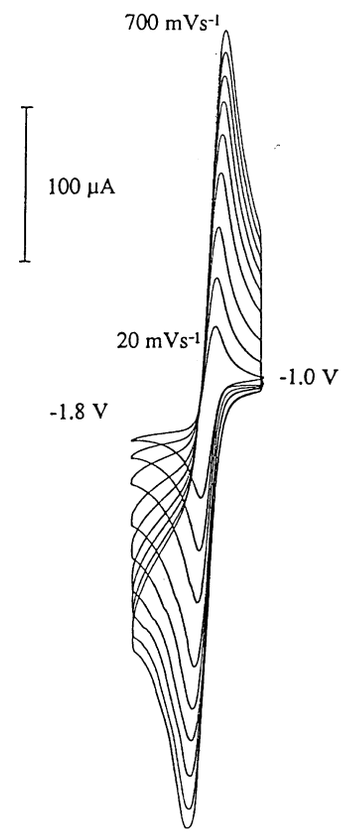

Fig. 5 Cyclic voltammogram recorded at a glassy carbon electrode (*vs.* SCE) for complex **3a** (*ca.* 1 mmol dm^{-3}) in CH_2Cl_2–$[NBu^n_4][BF_4]$ (*ca.* 0.2 mol dm^{-3}) as a function of scan rate (range 20–700 mV s^{-1}) at 254 K

are slightly longer than those in $[V(hida)_2]^-$ (range 0.14–0.02, average 0.094 Å). The η^2-NO groups subtend angles at tantalum which are similar to those in **1** (Table 2) and the planes of these two groups in each anion deviate from being mutually perpendicular (Δ,Λ 98.4, Λ,Δ 96.9°), but each {TaNO} plane is effectively perpendicular (Δ,Λ 92.9 and 89.1, Λ,Δ 88.91 and 90.6°) to the least-squares plane of the tantalum and the four carboxylate oxygen-donor atoms. As in **1** these oxygen atoms show similar displacement from this least-squares plane. For Δ,Λ O(6) and O(10) sit below (−0.43 and −0.39 Å, respectively) and O(1) and O(5) above (0.45 and 0.34 Å, respectively) and for Λ,Δ O(11) and O(15) sit above (0.46 and 0.37 Å, respectively) and O(16) and O(20) below (−0.38 and −0.45 Å, respectively) the plane, which contains the tantalum atom. The close similarity between the structures of **1** and **2** is not unexpected since the effective ionic radius of both niobium(v) and tantalum(v) is 64 pm.[20]

Compound **3a** exhibits the same Amavadin-style eight-coordination (Fig. 4), and was obtained as colourless, prismatic crystals in the space group $P2_12_12_1$ (Table 1). Refinement was carried out for the Λ helical form only. The *R*,*R* ligand can be used as a lock on the structure solutions since the chirality of the ligand is carried directly through to the complex. The Nb–O and Nb–N bond lengths are comparable to those in **1** and **2**, but slightly longer than in $[\Delta\text{-V}(S,S\text{-hidpa})_2]^-$ (range 0.12–0.06, average 0.08 Å) (Table 2). The η^2-NO groups subtend angles at the niobium which are comparable to those in **1** and **2**, and the related vanadium complex (Table 2). The angles between the planes of the {NbNO} groups deviate from being mutually perpendicular (95.8°), and are comparable to those in $[\Delta\text{-V}(S,S\text{-hidpa})_2]^-$ (94.3°).[4] As before, each of the {NbNO} planes is approximately perpendicular to the least-squares plane of the niobium and four carboxylate oxygen atoms (88.3, 87.6°). Again these oxygen atoms are distorted from the least-squares plane; O(1) and O(5) sit below (−0.36 and −0.45 Å), O(6) and O(10) above (0.37 and 0.53 Å) the plane containing the niobium atom.

Cyclic voltammetric studies

The redox properties of these Amavadin-style compounds have been investigated and the new niobium(v) and tantalum(v) species have revealed some novel reduction chemistry. Fig. 5 shows the cyclic voltammogram obtained for **3a** which exhibits a quasi-reversible redox couple at 254 K in CH_2Cl_2 ($E_{\frac{1}{2}} = -1.35$ V

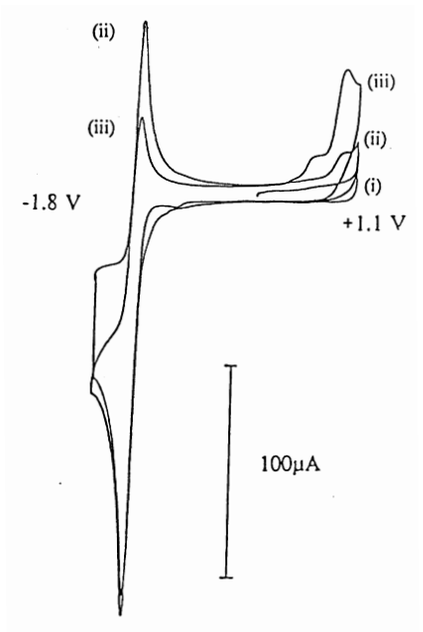

Fig. 6 Cyclic voltammogram recorded for complex **3a** at 298 K during a multiscan experiment in CH_2Cl_2 with a constant scan rate of 100 mV s^{-1} [see text for description of (i)–(iii)]

vs. SCE, $\Delta E = 110$ mV at 200 mV s^{-1}), showing a larger ΔE value compared to ferrocene ($\Delta E = 60$ mV) under identical conditions. The cathodic current peak (i_{pc}) intensity obeys a linear relationship with square root of the scan rate, between a range of 20 to 700 mV s^{-1}. Also, the ratio of the anodic current peak (i_{pa}) to the cathodic current peak (i_{pc}) remains approximately 1 : 1 during the same variable-scan-rate experiment (range 0.92–1.06 : 1). Under similar conditions at 298 K, $[PPh_4][V(hidpa)_2]$ exhibits a completely reversible V^{V}–V^{IV} redox couple at +0.10 V (*vs.* SCE),[5] and **1** also displays a similar quasi-reversible redox couple under identical conditions at 254 K ($E_{\frac{1}{2}} = -1.22$ V *vs.* SCE, $\Delta E = 140$ mV at 200 mV s^{-1}); i_{pc} obeys a linear relationship with the square root of the scan rate, however the $i_{pa} : i_{pc}$ ratio deviates from 1 : 1 (range 0.88–1.30 : 1).

In contrast complex **2** shows a completely irreversible reduction process at −1.92 V (*vs.* SCE). When the potential sweep of the cyclic voltammogram for **3a** was extended to +1.1 V and recorded at 298 K a new irreversible peak was observed at +1.0 V (*vs.* SCE). Fig. 6 shows the voltammograms obtained during a sequence of multiscan experiments for **3a**. In the initial sweep profile (i), with a sweep sequence of 0.0, +1.1, −1.8, 0.0 V, no peak is observed at the positive potential. Sweep (ii), the subsequent scan, showed a small peak at +1.0 V. During the final scan (iii), with a sweep sequence of 0.0, −1.8, +1.1, 0.0 V, the potential was held at −1.8 V for 30 s, and resulted in a decrease in the anodic peak intensity of the reduction process, followed by an increase in the intensity of the peak at +1.0 V. The new irreversible peak observed at +1.0 V in the multiscan experiment (Fig. 6) is attributed to the increased irreversible character of the reduction process of **3a** at 298 K. When this experiment was carried out for **3a** at 254 K no peak was observed at +1.0 V.

Compounds **1** and **3b** exhibited a similar set of voltammograms as that shown for **3a** (Fig. 6) under identical conditions. However, **2** showed an irreversible peak at +1.3 V even at 254 K, highlighting the enhanced instability of Ta^{IV} compared to that of Nb^{IV}. The voltammograms in Fig. 6 are consistent with an initial metal-based reduction process followed by a chemical reaction or rearrangement of **3a**, the product of which is detected by the new peak observed at +1.0 V. This behaviour contrasts with the redox properties of the related vanadium systems,[3] which exhibit a completely reversible one-electron V^{V}–V^{IV} couple, establishing that the metal(v), d^0 (M = Nb or Ta) species is highly favoured with these 4d and 5d metals. The molybdenum analogue showed a completely reversible Mo^{VI}–Mo^{V} redox couple in CH_2Cl_2 at 298 K[10] but this oxidation process was found to be irreversible in water at the same temperature,[11] highlighting the influence of solvent on the redox chemistry of these complexes.

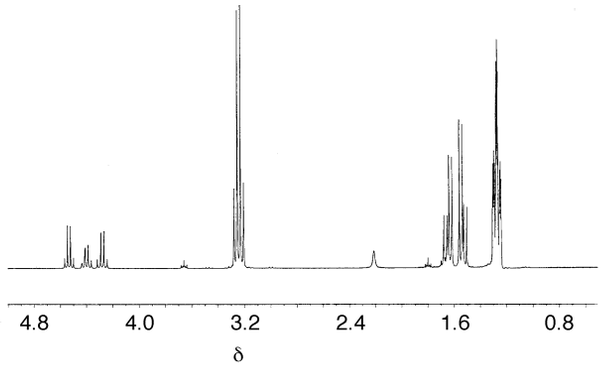

Fig. 7 Proton NMR (300 MHz, CD_2Cl_2, 298 K) spectrum of complex **3a**

Proton and ^{13}C NMR studies

Proton and ^{13}C NMR data have provided a valuable means of characterising these compounds. The anions $[ML_2]^-$ (M = Nb^{V} or Ta^{V}, L = hida or hidpa) are assigned C_2 point symmetry in solution on the basis of the crystallographic data and the NMR spectra observed, where the two-fold axis bisects the normals to the {MNO} plane from each ligand projected through the metal atom. The ^{1}H NMR spectrum obtained for **3a** (Fig. 7), is consistent with C_2 point symmetry for the eight-co-ordinate anion and the presence of both Λ and Δ helical forms in solution. There are four distinct environments for the methyl and methine protons (see Fig. 4). Fig. 7 shows three quartets at δ 4.54, 4.42 and 4.28 due to the methine protons (that at δ 4.42 is two quartets superimposed on one another) and four doublets at δ 1.68, 1.63, 1.56 and 1.52 (vicinal coupling, $^3J_{HH} = 8$ Hz) assigned to the methyl protons. A ^{1}H correlation spectroscopy (COSY) experiment on **3a** showed coupling of resonances at δ 4.54–1.56, 4.42–1.52, 4.42–1.68 and 4.28–1.63, respectively, which is comparable to that observed for the [Λ,Δ-V(*R*,*R*-hidpa)$_2$]$^-$ analogue.[5] Previous studies with the vanadium(v)–hidpa^{3-} complexes have included a comparison of the ^{1}H NMR spectrum observed for [Λ-V(*R*,*R*-hidpa)$_2$]$^-$ with that manifest by the Λ and Δ mixture of this complex.[5] Using these latter data and a comparison of integral intensities it is possible to assign the two superimposed quartets at δ 4.42 to the Λ form and the remaining resonances at δ 4.54 and 4.28 correspond to the Δ form. The integrals of these methine protons equate to approximately a 3 : 1 mixture of Δ to Λ in solution. A similar analysis of the integrals over the methyl resonances is consistent with this ratio, where δ 1.68 and 1.52 correspond to Λ form and the doublets at δ 1.63 and 1.56 to the Δ isomer. The overall concentrations of the two helical forms remain constant with respect to time, since a spectrum of **3a** taken 48 h later showed no change in the relative integrals. This is in contrast to the epimerisation reaction at vanadium which occurs over a comparable time-scale converting the Λ isomer into a 1 : 1 mixture of Δ and Λ.[5] However this epimerisation occurs for V^{IV} and not V^{V} implying an effect of the single unpaired electron in promoting the reaction hence the lack of reaction for the d^0 niobium(v) complex is not unexpected.

The ^{13}C NMR spectrum of complex **3a** displays four distinct environments for each type of carbon atom, listed in Table 3, also consistent with retention of two-fold symmetry in solution and the presence of both Λ and Δ helical forms. A similar comprehensive assignment for **3b** is difficult due to the complicated array of isomers giving rise to increased non-equivalence, as illustrated by the ^{13}C NMR data listed in Table 3. Complex

Table 3 Comparison of ^{13}C NMR (300 MHz, CD_2Cl_2, 298 K) resonances for complexes in **1**, **2**, **3a** and **3b**

	δ			
Compound	CO_2^-	CH	CH_2	CH_3
1	171.34		61.86	
	171.40		62.19	
2	172.82		60.69	
	172.93		60.88	
3a	173.62	63.74		12.62
	174.01	64.33		12.71
	175.29	67.77		14.51
	175.58	68.12		15.03
3b	173.96	68.11		12.83
	174.29	68.20		12.94
	174.37	68.29		14.82
	174.43	68.42		15.43
	174.52	68.57		16.44
	175.66	68.63		16.50

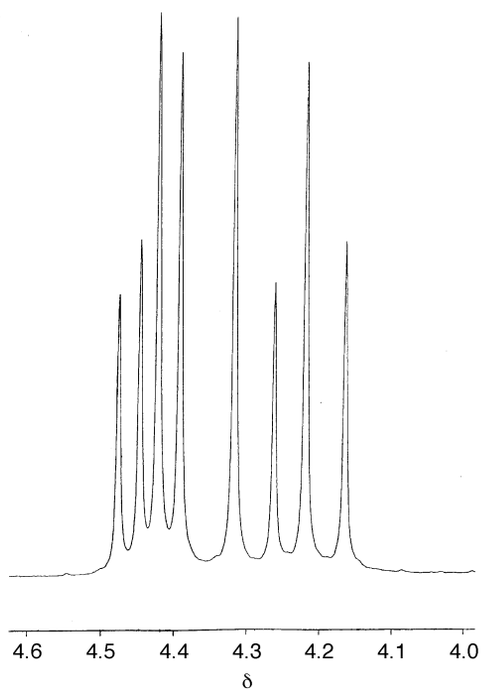

Fig. 8 Proton NMR (300 MHz, CD_2Cl_2, 298 K) spectrum of complex **2**

3b consists of three enantiomeric pairs which due to the C_2 point symmetry of $[Nb(R,S\text{-hidpa})_2]^-$ displays six carbon resonances in each region of the spectrum. The ^1H NMR spectrum emphasises this further where the peaks arising from the individual isomers overlap and appear as multiplets.

The ^1H NMR spectrum of complex **2**, shown in Fig. 8, displays four doublets at δ 4.45, 4.42, 4.29 and 4.19 (geminal coupling, $^2J_{HH} = -16$ Hz), consistent with the C_2 point symmetry of the eight-co-ordinate anion in solution. The Λ and Δ isomers each give rise to 2 × 2 doublets, but these species are enantiomers not diastereomers, so only four doublets are observed. Similarly in the ^{13}C NMR spectrum, where two separate resonances are present due to the carboxylate carbon atoms and in the methine region (Table 3). The ^1H–^{13}C correlation spectrum for **2** showed that the carbon resonance at δ 60.88 correlates to the doublets at δ 4.45 and 4.29 in the ^1H NMR spectrum and that at δ 60.69 carbon to the doublets at δ 4.42 and 4.19. The ^1H–^{13}C correlation spectrum corresponds to previous spectra obtained for $[PPh_4][V(hida)_2]$[6] and recent studies with analogous titanium and zirconium complexes.[21]

Table 4 Solvent effects on the ^{13}C NMR (300 MHz, 298 K) spectra of complexes **1**, **2** and **3b**

	δ (CO_2^-)	
Compound	CD_2Cl_2	D_2O
1	171.34–171.40	178.61–179.36
2	172.82–172.93	177.51–178.03
3b	173.96–175.66	179.25–181.21

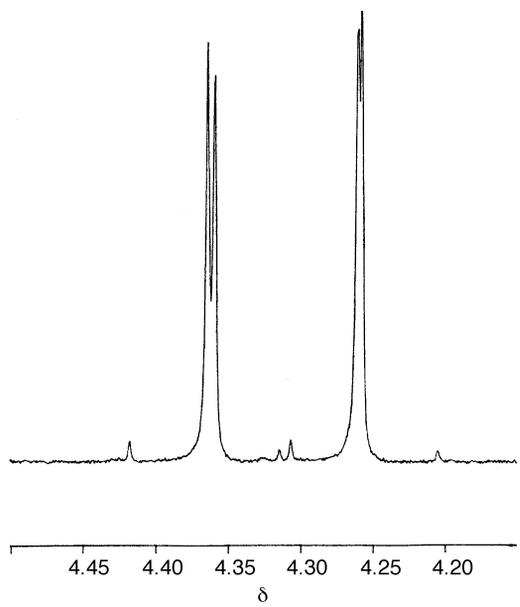

Fig. 9 Proton NMR (300 MHz, CD_2Cl_2, 298 K) spectrum of complex **1**

The ^1H NMR spectrum of complex **1** displays two pairs of resonances at δ 4.36 and 4.26, see Fig. 9. However, the ^{13}C NMR spectrum is comparable to the earlier examples showing two distinct environments in each of the carboxylate and methine regions (Table 3). The ^1H–^{13}C correlation spectrum for **1** shows that the carbon resonance at δ 62.19 correlates to the signals at δ 4.36 in the ^1H NMR spectrum and that at δ 61.86 correlates to the δ 4.26 resonances. These data are consistent with the loss of first-order status in the ^1H NMR spectrum, arising when the separation in resonance frequencies between the nuclei (Δν) approaches the line separation caused by the coupling $|J|$.[22] When the difference in chemical shift positions (Δν) is greater than $6|J|$ the multiplets are well separated and the distortion in line intensities is very slight and as the $|J|\Delta\nu$ ratio increases the line intensities are no longer equal. In the ^1H NMR spectrum obtained for **2** (Fig. 8), $\Delta\nu \approx 3|J|$, and a slight second-order distortion is observed where the inner lines are heightened. However, a more marked second-order distortion is seen in Fig. 9, where $\Delta\nu \approx 0.5|J|$, and overlapping of the signals occurs, although the outer (δ 4.42 and 4.20) and inner (δ 4.32 and 4.31) resonances are resolved.

Electrochemical studies of Amavadin[3] and the molybdenum analogue[10,11] have illustrated the influence of solvent on the oxidation/reduction potentials of the central metal ion of these complexes. For example, with Amavadin a shift of +500 mV is detected in the V^V–V^{IV} redox potential when switching from Me_2SO to aqueous conditions.[3] Recent X-ray crystallographic studies of Amavadin,[5] recrystallised from water, have shown that the unbound carboxylate oxygen atoms of the molecule link *via* hydrogen bonding to H_2O molecules forming a hydrogen-bonding network throughout the crystal lattice. This interaction *via* hydrogen bonding in solution has been explored further using ^{13}C NMR spectroscopy. The new compounds **1, 2** and **3b** provide an ideal means of investigating these solvent effects. Table 4 shows the ^{13}C NMR resonances of the carboxyl-

ate carbon atoms, recorded in CD_2Cl_2 and D_2O, where a downfield shift of δ 6–8 is observed, arising due to a deshielding effect on the carboxylate carbon atoms in the hydrogen-bonding enviroment.

Conclusion

The complexes **1**, **2**, **3a** and **3b** further establish the special mode of co-ordination adopted by *N*-hydroxydicarboxylate ligands *via* the η^2-NO group giving rise to a distinctive eight-co-ordinate geometry. Although $hida^{3-}$ and $hidpa^{3-}$ display a high affinity for vanadium, reactions with niobium and tantalum have confirmed that it is possible to replicate this co-ordination chemistry with other elements. The larger effective ionic radii of niobium(V) and tantalum(V) (64 pm) compared to vanadium(V) (54 pm) give rise to some subtle structural variations. There are no other related conventional co-ordination complexes with these metals in the literature, however, some tantalum complexes have been synthesised with iminoacyl ligands bound *via* an η^2-C,N group.[23] The geometries of the niobium and tantalum complexes are significantly different from those of the vandium complexes only with respect to the metal–ligand bond lengths. Electrochemical studies have highlighted the relative instability of the niobium(IV) and tantalum(IV) states, in contrast to the vanadium(IV) counterpart.

Acknowledgements

We thank British Nuclear Fuels PLC (BNF) for funding (to P. D. S. and S. M. H.), Dr. P. Harston (Company Research Laboratories, BNF, Springfields, Preston, Lancashire) and Mr. J. Friend (Department of Chemistry, The University of Manchester) for valuable discussions and assistance with NMR studies during the course of this work. D. C. thanks The Royal Society for financial support.

References

1 H.-U. Meisch, W. Reinle and J. A. Schmitt, *Naturwissenschaften*, 1979, **66**, 620.
2 E. Bayer and H. Kneifel, *Z. Naturforsch., Teil B*, 1972, **27**, 207.
3 M. A. Nawi and T. L. Riechel, *Inorg. Chim. Acta*, 1987, **136**, 33; J. J. R. Fraústo da Silva, M. F. C. G. da Silva, J. A. L. da Silva and A. J. L. Pombeiro, in *Molecular Electrochemistry of Inorganic, Bioinorganic and Organometallic Compounds*, eds. A. J. L. Pombeiro and J. A. McCleverty, Kluwer, Dordrecht, 1993, p. 411; E. M. Armstrong, S. N. Ertok, D. Collison and C. D. Garner, unpublished work.
4 E. M. Armstrong, R. L. Beddoes, L. J. Calviou, J. M. Charnock, D. Collison, S. N. Ertok, J. H. Naismith and C. D. Garner, *J. Am. Chem. Soc.*, 1993, **115**, 807.
5 E. M. Armstrong, M. S. Austerberry, D. Collison, S. N. Ertok, C. D. Garner, M. Helliwell and F. E. Mabbs, unpublished work.
6 E. M. Armstrong, L. J. Calviou, J. M. Charnock, D. Collison, S. N. Ertok, C. D. Garner, F. E. Mabbs and J. H. Naismith, *J. Inorg. Biochem.*, 1991, **43**, 413; L. J. Calviou, Ph.D. Thesis, University of Manchester, 1992.
7 E. Bayer, E. Koch and G. Anderegg, *Angew. Chem., Int. Ed. Engl.*, 1987, **26**, 545.
8 J. J. R. Fraústo da Silva, *Chem. Spec. Bioavail.*, 1989, **1**, 139.
9 M. A. A. F. de C. T. Carrondo, M. T. L. S. Duarte, J. C. Pessoa, J. A. L. da Silva, J. J. R. Fraústo da Silva, M. C. T. A. Vaz and F. L. Vilas-Boas, *J. Chem. Soc., Chem. Commun.*, 1988, 1158.
10 H. S. Yadav, E. M. Armstrong, R. L. Beddoes, D. Collison and C. D. Garner, *J. Chem. Soc., Chem. Commun.*, 1994, 605.
11 P. D. Smith, S. M. Harben, R. L. Beddoes, D. Collison and C. D. Garner, unpublished work.
12 J. Felcman, M. Cândida, T. A. Vaz and J. J. R. Fraústo da Silva, *Inorg. Chim. Acta*, 1984, **93**, 101.
13 E. Koch, H. Kniefel and E. Bayer, *Z. Naturforsch., Teil B*, 1986, **41**, 359; G. Anderegg, E. Koch and E. Bayer, *Inorg. Chim. Acta*, 1987, **127**, 183.
14 C. J. Pickett, *J. Chem. Soc., Chem. Commun.*, 1985, 323.
15 R. R. Gagné, C. A. Koval and G. C. Lisensky, *Inorg. Chem.*, 1980, **19**, 2854.
16 N. Walker and D. Stewart, *Acta Crystallogr., Sect. A*, 1983, **39**, 158.
17 G. M. Sheldrick, SHELXS 86, *Crystallographic Computing 3*, eds. G. M. Sheldrick, C. Krueger and R. Goddard, Oxford University Press, 1986.
18 D. T. Cromer and J. T. Waber, *International Tables for X-Ray Crystallography*, Kynoch Press, Birmingham, 1974, vol. 4, Tables 2.2A and 2.3.1.
19 TEXSAN-TEXRAY Structure Analysis Package, Molecular Structure Corporation, Houston, TX, 1985.
20 R. D. Shannon, *Acta Crystallogr., Sect. A*, 1976, **32**, 751.
21 S. M. Harben, P. D. Smith, R. L. Beddoes, D. Collison and C. D. Garner, unpublished work.
22 W. Kemp, *NMR in Chemistry*, Macmillan Education, London, 1986, p. 75; R. K. Harris, *Nuclear Magnetic Resonance Spectroscopy*, Pitman Books, London, 1983, p. 47.
23 L. R. Chamberlain, L. D. Durfee, P. E. Fanwick, L. Kobriger, S. L. Latesky, A. K. McMullen, I. P. Rothwell, K. Folting, J. C. Huffman, W. E. Streib and R. Wang, *J. Am. Chem. Soc.*, 1987, **109**, 390; J. R. Clark, P. E. Fanwick and I. P. Rothwell, *J. Chem. Soc., Chem. Commun.*, 1993, 1233.

Received 19*th August* 1996; *Paper* 6/05750K